ELSEVIER

Polymer 42 (2001) 6759–6764

polymer

www.elsevier.nl/locate/polymer

The effect of concentration on the rate of formation of liquid crystal and crystalline phases

I.J. McEwen, S.W. Watt, C. Viney*

Department of Chemistry, Heriot-Watt University, Riccarton, Edinburgh EH14 4AS, Scotland, UK

Received 22 January 2001; accepted 26 February 2001

Abstract

In certain instances the rates of growth of a lyotropic phase from isotropic solutions of biological polymers is observed to be concentration dependent. Such behaviour is rationalised in this paper by treating lyotropy as a nucleated phenomenon and by considering the free energy requirements of stable nuclei. The relative number of stable nuclei from which phase growth can occur depends on both the free energy and the interfacial energy differences between the isotropic and the anisotropic state. Adopting the Flory lattice approach to quantify the former, and using a realistic value for the latter, an expression is derived which predicts that the rate of phase formation passes through a maximum as the concentration of the isotropic solution is increased. This result is analogous to the time–temperature relation that describes nucleated solidification and solid-state transformations in metals. The conditions under which mesogen crystallisation will occur are also discussed in terms of the relative rate of nucleation for this process compared with that of liquid crystal formation.

Keywords: Phase transformation kinetics; Liquid crystal nucleation; Free energy

1. Introduction: time dependent transformations

The conversion of one phase into another requires that both thermodynamic and kinetic parameters be favourable. The familiar Time–Temperature–Transformation (TTT) curves, which are commonly plotted for metallurgical systems [1], provide a practical demonstration of the interplay of the temperature dependencies of the free energy governing nucleation and the kinetics of phase growth. Fig. 1(a) shows a schematic TTT diagram with its typical C-shape for the transformation of phase A into another phase B. The usually observed situation is one in which a metal or alloy, at a temperature above the equilibrium one for the existence of phase B, is quenched below that temperature, e.g. along line $p \rightarrow q$ in the figure. A period of time usually elapses ($q \rightarrow r$) before the first appearance of phase B at r; conversion then evolves over time $r \rightarrow r'$ and is complete, or at least observably complete, at time r'.

C-curves result from a nucleation and growth mechanism [2]. At temperatures just below the equilibrium line the lapse time ($q \rightarrow r$) is relatively long, since here the thermodynamic drive for nucleation is small and the overall transformation is consequently slow. At higher undercoolings this driving force increases and transformation becomes more rapid. Eventually however, at very high undercoolings, diffusion becomes the limiting factor and the whole process slows again.

In previous publications [3,4] one of us (C.V.) reported that the formation of lyotropic liquid crystalline phases by three biological polymers — silk fibroin (a protein), levan (a polysaccharide) and mucin (a glycoprotein) — conforms to a very similar pattern but where the vertical axis is now concentration as shown in Fig. 1(b). The equilibrium line now defines the minimum concentration for the existence of a liquid crystalline phase, i.e. it is the saturation limit for the isotropic solution. Phase A areas, respectively above and below this saturation line, correspond to isotropic and to supersaturated isotropic solutions, and the phase B area corresponds to the anisotropic lyotropic liquid crystalline phase. In this case a solution, initially at p, rapidly loses solvent and arrives at q; lyotropy is first observed at r and the volume fraction of liquid crystalline phase B then increases with time along line $r \rightarrow r'$. Fig. 1(b) thus represents a Time–Concentration–Transformation (TCT) curve. Such phase behaviour, as a function of concentration, presents obvious similarities to the time-dependent temperature-driven phase changes in bulk metals and alloys. Conceptually, both systems are responding to the same

* Corresponding author. Tel.: +44-0131-451-3759; fax: +44-0131-451-3180.

E-mail address: c.viney@hw.ac.uk (C. Viney).

0032-3861/01/$ - see front matter
PII: S0032-3861(01)00168-9

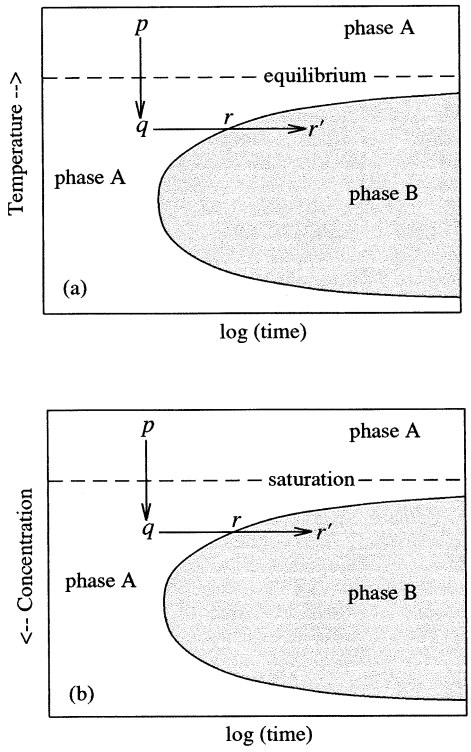

Fig. 1. (a) Schematic time–temperature behaviour for the transformation of phase A (unshaded) into phase B (shaded). Phase A is stable above the equilibrium line, phase B is stable below the equilibrium line. See text for further details. (b) Schematic time-composition behaviour for the transformation of isotropic phase A (unshaded) into an anisotropic phase B (shaded). Phase A is stable above the saturation line, phase B is stable below the saturation line. See text for further details.

processes, nucleation and a subsequent growth stage, and in this communication we propose a semiquantitative rationale for the observation of TCT behaviour in lyotropic polymer solutions.

2. A simple model for Time–Concentration–Transfomation behaviour

2.1. Thermodynamics of phase transformation

First consider the free energy of mixing for two liquids where component 1 is a solvent and component 2 is the *unordered* mesogenic solute. Such a situation can be represented by curve *a* in Fig. 2, although the terminus at volume fraction $v_2 = 1$ on this curve could represent a hypothetical condition since the undiluted mesogen may not exist as an unordered phase at temperatures of interest. Curve *b* is drawn to represent the free energy change which results on producing an *ordered* anisotropic solution. The terminus of this second curve at $v_2 = 1$ is placed at a lower free energy with respect to the isotropic state, where it represents a solvent-free ordered anisotropic liquid state; the difference ΔG^* should correspond to an isotropic–anisotropic transi-

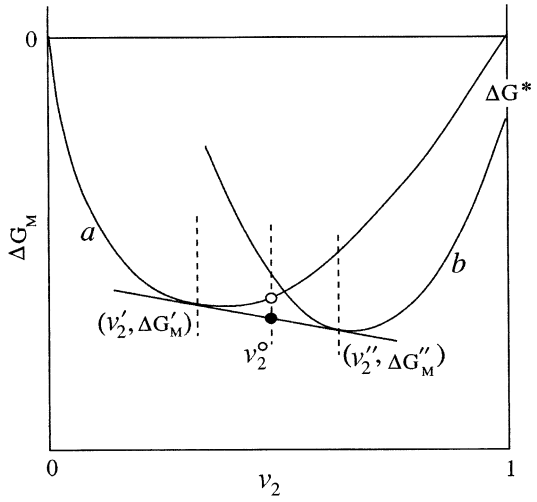

Fig. 2. Schematic free energy of mixing curves for (a) an isotropic mixture and (b) an anisotropic mixture as a function of the volume fraction v_2. See text for further details and explanation of symbols.

tion of the type observable in thermotropic liquid crystal substances. Curve *b* effectively terminates at some finite value of $v_2 > 0$, towards the left of the diagram, since lyotropic liquid crystalline behaviour is limited to relatively concentrated solutions. A common tangent line to curves *a* and *b* contacts the former at $v_2{}'$ and the latter at $v_2{}''$, where the free energies are $\Delta G'_M$ and $\Delta G''_M$ respectively.

Consider a solution initially on curve *a* at a volume fraction less than $v_2{}'$. Let this solution lose solvent rapidly, arriving at a composition between $v_2{}'$ and $v_2{}''$ such as the one shown by the open circle at v_2^0. Now, given that there is an effective coupling between the two free energy curves, this solution has the opportunity to reduce its free energy by separating into two phases: an isotropic phase with composition $v_2{}'$ on curve *a* and an anisotropic liquid crystalline phase with composition $v_2{}''$ on curve *b*. The arguments for this are exactly those applicable to phase boundaries of binary liquid mixtures which are defined on a single (continuous) free energy curve [5]. However, the system depicted in Fig. 2 differs from such mixtures in that the free energy curves for the isotropic and anisotropic phases are not joined into a single curve. Indeed, they cannot be [6], because the isotropic and anisotropic phases are structurally distinct. Spinodal conditions are therefore absent, i.e. there is no region over which $d^2\Delta G_M/dv_2^2 < 0$ (concave 'downwards') and where compositional fluctuations can reduce the free energy and lead to phase separation via a purely diffusion controlled process. Phase separation here can only occur by nucleation and growth, and so, for the resulting two-phase system at v_2^0 in Fig. 2, the total free energy will be

$$\Delta G_M^0 = \Phi' \Delta G_M^{'} + \Phi'' \Delta G_M^{''}, \quad (1)$$

where Φ' and Φ'' are the volume fractions of the two coexisting phases. ΔG_M^0 is then readily shown [5] to be the

value of the free energy at the point of intersection of the common tangent with composition v_2^0 indicated by the filled circle in Fig. 2. The description of the isotropic/liquid crystal phase transition as a nucleation and growth process is supported by experiment [7,8].

For all compositions between v_2' and v_2'', therefore, we may take the difference between curve *a* and the common tangent as a measure of the free energy accompanying the formation of an anisotropic liquid crystalline phase from an isotropic solution. v_2' is the minimum composition for the formation of liquid crystalline phase and the volume fraction of this phase increases from zero at v_2' to unity at v_2''. This treatment does not address how the isotropic and anisotropic states are coupled in statistical mechanical terms; it is only concerned with net free energy differences. Isotropic solutions on curve *a* at concentrations greater than v_2'' are also unstable, but with respect to a single ordered phase only. However, the continuation of these free energy curves to high concentrations may represent a purely hypothetical situation since crystallisation of the mesogen could intervene at some point.

The composition dependence of the free energy difference between an anisotropic and an isotropic mixture (ΔG_{a-i}) may be stated formally as

$$\Delta G_{a-i}/RT = [x_1(\mu_1 - \mu_1^0) + x_2(\mu_2 - \mu_2^0)]_a - [x_1(\mu_1 - \mu_1^0) + x_2(\mu_2 - \mu_2^0)]_i. \quad (2)$$

The chemical potentials for the solvent (1) and the mesogen (2) under both isotropic and anisotropic conditions were derived by Flory in the 1950s from his lattice treatment of such systems. Using the Flory prescriptions [9,10] for these leads to the following result:

$$\Delta G_{a-i}/RT = x_1[v_2\{(y/x) - 1\} + 2/y] - x_2[v_2(y - x) + 2\ln(x/y) + 2], \quad (3)$$

where v_2 as before is the overall volume fraction of mesogen and x_1 and x_2 are the mole fractions of solvent and mesogen, respectively. The solvent occupies one lattice site and the mesogen occupies x, so that x is also the axial (length-to-width) ratio. The parameter y was introduced by Flory as a disorientation index and is related to v_2 through

$$v_2 = [x/(x - y)][1 - \exp(-2/y)]. \quad (4)$$

The limitations of using y to characterise disorientation were recognised by Flory [11] and others [12], but it provides a robust first approximation from which to proceed with a simple model, provided that y and x are assigned physically realistic values.

Fig. 3 shows results obtained from Eqs. (3) and (4) for $x = 25$ and 50. These calculated data represent an athermal system and embody the strictures and limitations of the lattice approach which considers only 'hard' interactions; however, they confirm the free energy difference to be an increasingly negative function of the supersaturation

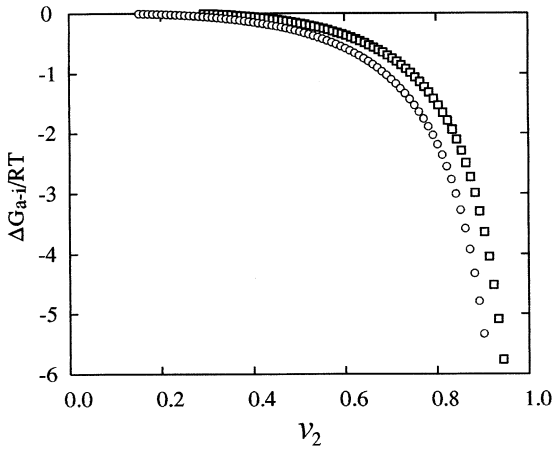

Fig. 3. Calculated free energy difference (ΔG_{a-i}) between an isotropic mixture and the corresponding anisotropic mixture as a function of the solvent volume fraction v_2 according to Eqs. (3) and (4). Squares are for an axial ratio of 25, circles for an axial ratio of 50.

of the isotropic solution, and in this light it is possible to address the concentration dependence of nucleation thermodynamics.

2.2. Concentration-dependent nucleation

We consider that small elements of anisotropic phase, arising from thermal or density fluctuations, can act as nuclei for further growth and that these respond to two competing effects: a favourable contribution from ΔG_{a-i} proportional to the volume of the element, and an unfavourable surface energy contribution proportional to its surface area. An equation describing this for the case of a spherical nucleus is [2]:

$$\Delta G_r = 4/3\pi r^3 \Delta G_{a-i} + 4\pi r^2 \gamma, \quad (5)$$

where ΔG_r is the free energy of a nucleus of radius r. ΔG_{a-i} here is scaled per unit volume and γ is the interfacial free energy per unit area. For values of ΔG_{a-i} less than zero, the classical Eq. (5) posseses a maximum which defines a critical size r_c and a critical free energy ΔG_c as shown in Fig. 4.

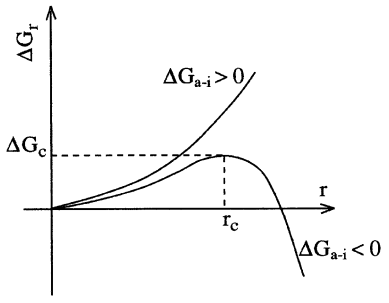

Fig. 4. Relation between the total free energy of an anisotropic nucleus (ΔG_r) and its radius (r) according to Eq. (5) for positive and negative values of the free energy difference ΔG_{a-i}. See text for explanation of other symbols.

Nuclei larger than r_c are deemed stable sites at which growth will occur (thereby reducing the overall free energy of the nucleus), whereas those smaller than r_c are not viable and will disappear. ΔG_c and r_c are both functions of the driving force ΔG_{a-i}, itself a function of concentration through Eq. (3). Differentiation of Eq. (5) gives r_c which, when substituted back, defines

$$\Delta G_c = 16\pi\gamma^3/3(\Delta G_{a-i})^2 \quad (6)$$

as the critical free energy for the formation of a viable nucleus. The inverse proportionality between ΔG_{a-i} and ΔG_c means that the latter is a positive but decreasing function of the concentration v_2 of the isotropic solution in which the nuclei form. The equilibrium between the number of critical nuclei n_c (size r_c) and the total number of nuclei (N) is

$$n_c/N = \exp(-\Delta G_c/kT) \quad (7)$$

and so the relative proportion of viable nuclei at which phase growth can proceed will increase with v_2. Viable nuclei cannot form for v_2 less than v_2'.

2.3. Nucleation and growth

Growth of a viable nucleus should depend on the mobilities of both mesogen and solvent as they adopt their more ordered states. For rods of finite thickness, the theory of Edwards and Evans [13] provides an expression for the concentration effect on the diffusion coefficient, which can be usefully approximated by an exponential. Diffusion of solvent molecules is impeded as concentration increases and this also has been found to decrease in an exponential manner [14]. Rather than attempt to model what must necessarily be a complex transport process we suggest that a generalised 'global' diffusion or transport term (D) should adequately describe the concentration dependance of accretion at the surface of a growing nucleus and we choose an overall exponential dependence

$$D = D_0 \exp(-\beta v_2), \quad (8)$$

where β and D_0 are system constants. Phase B growth will be proportional to both the number of critical nuclei and to the rate of transport so that we may combine Eqs. (7) and (8) to give the following description of the overall rate (I) as a function of the solution composition v_2:

$$I \propto D_0 N \exp[-\beta v_2 - \Delta G_c(v_2)/kT]. \quad (9)$$

Relationship (9) can be evaluated. The calculated $\Delta G_{a-i}/RT$ curves shown in Fig. 3 refer to a mole of mixture of solvent and mesogen whose molar volumes are defined by the choice of the size of a lattice site. We have adopted a representative volume of 100 cm^3 per mole of lattice sites to reexpress ΔG_{a-i} in J cm^{-3}. Eq. (6), with an appropriate value for the interfacial energy γ, will then provide the necessary values of ΔG_c as a function of v_2. The interfacial energy for a system of hard rods has been calculated by Doi and Kuzuu

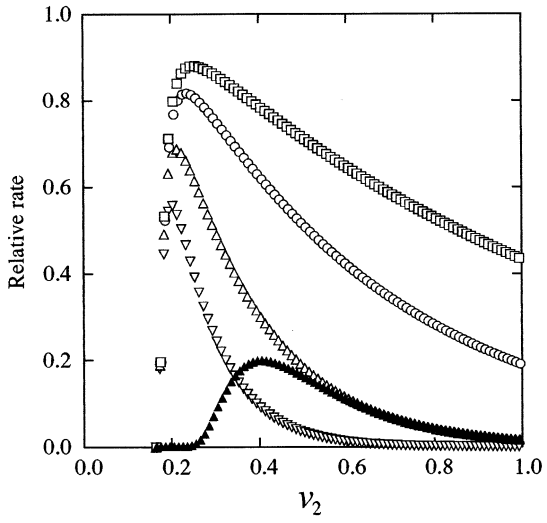

Fig. 5. The relative rate of lyotropic phase growth as a function of volume fraction v_2 according to Eq. (9) calculated as detailed in the text. Open symbols are for $\gamma = 0.2 \times 10^{-8}$ J cm^{-2} with $\beta = 10$ (inverted triangles), $\beta = 5$ (triangles), $\beta = 2$ (circles) and $\beta = 1$ (squares). Filled triangles are for $\beta = 5$ and $\gamma = 10^{-8}$ J cm^{-2}.

[15] who obtained $\gamma = 0.11 \times 10^{-8}$ J cm^{-2}. Experimental values are slightly greater than this; Faetti and Palleschi [16] reported the range $0.07–0.18 \times 10^{-8}$ J cm^{-2} for cyanobiphenyls and Williams [17] found $\gamma = 0.16 \times 10^{-8}$ J cm^{-2} for *N*-(*p*-methoxy benzylidene)-*p*-butylaniline (MBBA). Chen et al. [18] obtained a value of 0.24×10^{-8} J cm^{-2} for poly(*n*-hexyl isocyanate) using the pendant drop method and further suggested that chain flexibility may account for the discrepancy between theory and experiment. We have thus chosen $\gamma = 0.2 \times 10^{-8}$ J cm^{-2} as a reasonable value for the interfacial energy between an isotropic and an anisotropic phase and have evaluated the exponential term on the right hand side of relationship (9) for various values of the diffusion exponent β to obtain the curves shown in Fig. 5. These describe the relative rate of phase B formation as a function of concentration v_2 for a mesogen of axial ratio 50.

The rate rises steeply from zero at $v_2' = 0.15$, the saturation limit for an axial ratio of 50, where it is thermodynamically controlled by the increasing availability of nuclei. It passes through a maximum and then decreases as diffusion becomes the limiting factor. The inverse of rate, the time for the appearance of observable amounts of lyotropic phase B, will then exhibit the typical C-shape which is illustrated in Fig. 1(b), the 'nose' of the resulting TCT curve corresponding to the maximum in the rate. The concentration at which the maximum occurs responds somewhat weakly to β (we have varied this parameter by a factor of 10), which can be seen to have a greater controlling effect on the width of the rate peak. The position of the peak is much more sensitive to the value of γ; in Fig. 5 the calculated maximum moves from $v_2 \sim 0.25$ to $v_2 \sim 0.4$ when γ is increased to 1.0×10^{-8} J cm^{-2}. For values of

$\gamma > 10^{-7}$ J cm^{-2} the maximum moves unrealistically close to $v_2 = 1$.

Our adoption of the exponential form, Eq. (8), to describe the diffusion process is a reasonable choice [13,14] in systems containing polymeric solutes such as those [3,4] which prompted us to develop this treatment. A similar picture emerges if, instead of an exponential diffusion dependence, other dependences are chosen, such as the inverse power law found to describe the diffusion of poly-(benzyl glutamate) [19]. All that is required is that the mass transport rate is decreased with increased concentration. For non-polymeric solutes, transport should be less sensitive to concentration, i.e. β will be small, and in such cases C-type behaviour may not be observable. There appears to be no data in the literature which would give a reliable guide to a value of β characteristic of transport–concentration effects in lyotropic solutions and so the data in Fig. 5 are shown calculated for a plausible range of values. Nevertheless, given the proposed kinetic and thermodynamic preconditions, the foregoing arguments do rationalise the existence of C-curve behaviour in lyotropic systems undergoing a concentration increase. The analogy with a TTT profile, though close, cannot be made completely. The concentration analogue of a near instantaneous temperature quench, the trajectory $p \rightarrow q$ shown in Fig. 1(b), could never be achieved in practice since instantaneous solvent loss from a macroscopic sample is quite impossible, as is the absence of concentration gradients during solvent loss. Fig. 6 shows a much more realistic trajectory for more gradual solvent loss. The system becomes metastable with respect to the liquid crystal phase at q but lyotropy is not observed until higher concentrations and later times at r.

2.4. Crystallisation

At high enough concentrations solidification of the mesogen is quite likely, but again both kinetic and thermodynamic parameters will dictate events. This is illustrated by the observation that various natural materials show a structural organisation which is reminiscent of liquid crystalline phases, a subject which has been eloquently discussed by Ciferri and Krigbaum [20] who suggest that solidification occurs via a precursor liquid crystalline state rather than directly from an isotropic solution. These authors [21] adopted a modification of the well-known Flory depression of melting point expression [22] to describe the concentration–temperature equilibrium between a crystalline and a liquid crystalline phase. So, within the context of our present discussion of isothermal C-curve behaviour, we should allow for a second possible equilibrium to be included in Fig. 6 below which the anisotropic solution is saturated with respect to a crystalline phase. Following the phase diagrams presented by Ciferri and Krigbaum [20], and also arguments proposed by Papkov [23] on the same topic, we conclude that this most likely lies at higher concentrations than that for the onset of liquid crystallinity as shown by line 2 in the figure. For solutions of greater concentration than this, the most stable thermodynamic state of the system is crystallized mesogen in equilibrium with its saturated anisotropic solution.

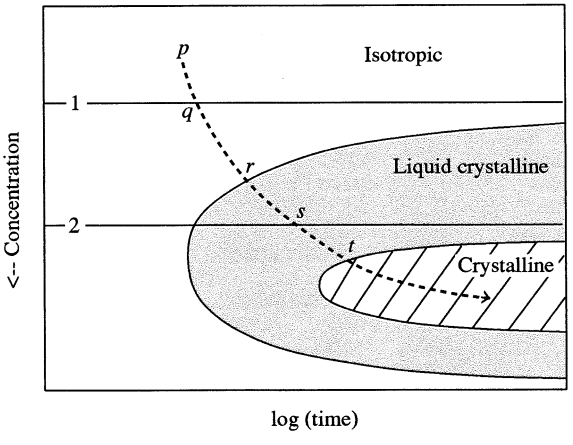

Fig. 6. Schematic TCT diagram describing phase behaviour as a function of solvent loss. Lines 1 and 2 respectively represent the saturation concentrations above which the liquid crystalline and crystalline phases are thermodynamically stable. See text for further explanation.

The question then can be asked: which phase, crystal or liquid crystal, will form when a solution is rapidly brought to crystalline saturation? Since crystallisation is also a nucleated process, both this and liquid crystalline phase formation will compete in terms of the relative numbers of critical nuclei available for each of these phases. Eq. (5) also applies to a crystal nucleus [2] and consideration of the interfacial energy term suggests that crystal nucleation will be the less favoured process. This can be usefully demonstrated under the conditions that correspond to the maximum of the $\beta = 5$ curve in Fig. 5. The maximum occurs at $v_2 \sim 0.25$, where ΔG_{a-i}, from Eqs. (3) and (4), is of the order -10^{-2} J cm^{-3}. Using our value of $\gamma = 0.2 \times 10^{-8}$ J cm^{-2}, and evaluating Eq. (6) with a nucleus of nominal radius $\backsim 20 \times 10^{-8}$ cm, the critical free energy ΔG_c turns out to be of the order 10^{-22} J per nucleus.

Higher values of interfacial energy characterise solid–liquid interfaces. For example, the aqueous interface with nylon may be estimated [24] at $\gamma \sim 5 \times 10^{-7}$ J cm^{-2}. For crystallising biological macromolecules, surface hydration may alleviate interfacial effects somewhat; however, it would seem reasonable that γ values will be at least an order of magnitude greater that those of liquid crystalline interfaces. Retaining ΔG_{a-i} at the above value of -10^{-2} J cm^{-3}, but now setting γ to 2×10^{-8} J cm^{-2}, leads to ΔG_c of the order 10^{-19} J per nucleus and so the ratio n_c/N (Eq. (7)) is thus vanishingly small. For comparable values of the free energy for formation of the more ordered phase, therefore, liquid crystal nucleation is by far the more favoured process.

A likely scenario is shown by continuing the trajectory $p \rightarrow q \rightarrow r$ in Fig. 6, representing the further loss of solvent from the anisotropic liquid. The liquid crystalline phase is

thermodynamically stable until point *s* after which it is metastable with respect to crystallisation. For kinetic reasons, however, crystallisation does not occur until longer timescales, and not until point *t* is reached does it pass over into an ordered solid state represented by the hatched area in the figure — provided of course the alternative of vitrification does not occur. The whole trajectory, from isotropic liquid at *p* through the liquid crystal region from *r* to *t* and onwards through the crystalline region, represents the non-instantaneous solvent loss that is realised in real systems and encapsulates the ideas expressed by Ciferri and Krigbaum [20] of liquid crystallinity as a possible structure-defining precursor state to the organised crystalline solids found in Nature.

2.5. Effect of a finite rate of concentration change

Our present treatment is, as noted in the introduction, a semi-quantitative rationale for the observation of TCT behaviour. Although the history of a drying sample is repesented by a continuous trajectory such as $p \rightarrow t$ in Fig. 6, the C-shaped transformation curves themselves assume that material is instantaneously brought to a supersaturated concentration and then allowed to undergo microstructural change. In other words, the transformation curves suppose that concentration of the *bulk* isotropic system is changed rapidly by the removal of solvent; subsequent *local* rearrangement of concentration needed to produce new phases is limited by polymer diffusion, and the progress of this local rearrangement is charted along the horizontal axis of the plot. The isothermal metallurgical TTT curves that served as the inspiration for our model are constructed on the basis that the transformation temperature is reached instantaneously. A more refined — but necessarily more complex — approach constructs curves on the basis of continuous finite rates of system temperature decrease, leading to C-shaped 'Continuous Cooling Transformation' curves [25]. An analagously sophisticated treatment for concentration change will require extensive experimental input, and will be described in a future publication.

3. Conclusions

Some biological polymers exhibit a time and concentration dependence on forming a lyotropic liquid crystalline phase from aqueous solution. Using the analogy of time–temperature dependence shown in metallurgical phase transformations we have developed a first-order description of this process which considers the formation of liquid crystallinity to be a nucleated phenomenon dependant on the free energy difference between the phases and on the interfacial energy at the phase boundary. The Flory lattice theory is used to describe the concentration effect on the free energy difference between an anisotropic and an isotropic phase, and expressions are then derived which predict the rate of lyotropic phase formation by considering the number of stable nuclei and a diffusion limited transport contribution. Using literature values of the interfacial energy, the rate is shown to go through a maximum at a certain concentration which is in accord with the observed time–concentration behaviour. Crystallisation of an anisotropic phase is also considered and by using parallel arguments this also should show time–concentration behaviour.

Acknowledgements

We gratefully acknowledge Heriot-Watt University for supporting SWW through the award of a studentship.

References

[1] Boyer H, editor. Atlas of isothermal transformation and cooling transformation diagrams. Cleveland, OH: American Society for Metals, 1977.
[2] Christian JW. In: Cahn RW, editor. Physical metallurgy. Amsterdam: North-Holland, 1965. p. 451.
[3] Viney C, Huber AE, Dunaway DL, Kerkam K, Case ST. ACS Symp Ser 1994;544:120.
[4] Viney C, Huber A, Verdugo P. In: Ching C, Kaplan DL, Thomas EL, editors. Biodegradable polymers and packaging. Lancaster, PA: Technomic Publishing Company, 1993. p. 209.
[5] Fernández ML. Science Progress 1990;74:257.
[6] Cottrell A. An introduction to metallurgy. London: Arnold, 1975. p. 227.
[7] Cheng SZD, Lee SK, Barley JS, Hsu SLC, Harris FW. Macromolecules 1991;24:1833.
[8] Lin J, Wu H, Li S. Polym Int 1994;34:141.
[9] Flory PJ. Proc Royal Soc Lond 1956;A234:73.
[10] Flory PJ. Adv Polym Sci 1984;59:1.
[11] Flory PJ, Ronca G. Mol Cryst Liq Cryst 1979;54:289.
[12] Chick LA, Viney C. Mol Cryst Liq Cryst 1993;226:41.
[13] Edwards SF, Evans KE. Trans Faraday Soc 1982;78:113.
[14] Mustafa MB, Tipton DL, Barkley MD, Russo PS, Blum FD. Macromolecules 1993;26:370.
[15] Doi M, Kuzuu N. J Appl Polym Sci, Polym Symp 1985;41:65.
[16] Faetti S, Palleschi V. J Chem Phys 1984;81:6254.
[17] Williams R. Mol Cryst Liq Cryst 1974;35:349.
[18] Chen WL, Sato T, Teramoto A. Macromolecules 1996;29:4283.
[19] Bu Z, Russo PS, Tipton DL, Negulescu II. Macromolecules 1984;27:6871.
[20] Ciferri A, Krigbaum WR. Mol Cryst Liq Cryst 1981;69:273.
[21] Ciferri A, Krigbaum WR. J Polym Sci, Polym Lett Ed 1980;18:253.
[22] Flory PJ. J Chem Phys 1949;17:223.
[23] Papkov SP. In: Pierce EM, Schaefgen JR, editors. Contemporary topics in polymer science. New York: Plenum Press, 1977.
[24] van Krevelen DW. Properties of polymers. New York: Elsevier, 1976. Chapter 8.
[25] Reed-Hill RE. Physical Metallurgy Principles. New York: van Nostrand Reinhold, 1964. Chapter 17.